

Monte Carlo Simulations of Liquid Hydrogen Fluoride¹

William L. Jorgensen

Contribution from the Department of Chemistry, Purdue University,
West Lafayette, Indiana 47907. Received April 3, 1978

Abstract: An intermolecular potential function for the hydrogen fluoride dimer determined from quantum mechanical calculations has been used in Monte Carlo simulations of liquid hydrogen fluoride at 0 °C. The structure of the liquid is elucidated from radial and energy distribution functions, coordination numbers, and drawings of polymeric aggregates. The liquid contains winding, hydrogen-bonded chains which run in alternate directions. The distribution functions indicate that a continuum of energetic environments are experienced by the hydrogen fluoride molecules. Thermodynamic properties, particularly the internal energy, energy of vaporization, heat capacity, and dielectric constant, were also calculated and are compared with the available experimental data. Several computational issues are discussed including the general applicability of Monte Carlo calculations to dipolar liquids with large dipole moments. Similar to a previous study of dipolar hard spheres, the results are found to depend noticeably on whether the spherical cutoff (SC) or minimum image (MI) convention is used in evaluating the intermolecular interactions. However, the dependence of the results on sample size in the SC calculations is small. Comparisons between liquid HF and water are stressed.

I. Introduction

Theoretical methods and computational facilities have now evolved sufficiently to enable the simulation of molecular liquids. It is not surprising that the initial studies have focused on the structure and thermodynamic properties of liquid water due to its biochemical significance.³⁻⁸ Some key works in this area are the molecular dynamics calculations of Rahman and Stillinger,⁴ the development of a water-water potential function from configuration interaction calculations by Matsuoka et al.,⁵ and the use of the function in Monte Carlo (MC) simulations by Clementi,⁶ Scheraga,⁷ and Beveridge⁸ and co-workers. The computations are arduous enough so that few studies of pure molecular liquids other than water have been reported: molecular dynamics for NH₃, CO, N₂, and recently HF⁹ and a MC calculation for benzene using a relatively crude potential function.¹⁰ Consequently, the general applicability and limits of such theoretical endeavors are not firmly established. In fact, the MC method has primarily been used to study fluids with much weaker attractive interactions than hydrogen bonding, for example, noble gas liquids³ and dipolar spheres with small (<ca. 1.5 D) dipole moments.¹¹

The results of Monte Carlo simulations of liquid hydrogen fluoride are presented here. Comparisons of liquid HF and water are intriguing for several reasons including the fact that although the dipole moments of HF and H₂O monomers are nearly identical (1.82 and 1.85 D), a structure containing chains of hydrogen-bonded monomers is anticipated for HF(l) as compared to the three-dimensional network of water. In addition, this work permits further assessment of the utility of MC calculations for modeling such cohesive fluids. Liquid HF is also fundamentally interesting as a solvent because its nonnucleophilic character allows the support of free carbonium ions.¹² Thus, the present study may lead to future modeling of the solvation of carbonium ions in superacid media.

To begin, an elementary review of the Monte Carlo method is presented since the procedure is not generally familiar to other than physical chemists. It is anticipated that the method will find applications in many areas particularly organic chemistry. The material in the next section may be skipped by readers knowledgeable in MC methodology. Sophisticated presentations are available elsewhere.^{3,13} The computational details of the present work are then described followed by the results and discussion.

II. The Monte Carlo Method

Two main features of the computational procedure are due to Metropolis et al.¹⁴ The first is the use of "periodic boundary

conditions" by which the liquid to be modeled is considered to be composed of duplicate images of a basic cube or other solid containing a fixed number, N , of solvent (and solute) molecules. This is, of course, reminiscent of the role of a unit cell in crystallography. For the treatments of water, N has been in the range 27-343 with values around 100 typical.^{3,6-8} The advantages of this procedure are the reduction of a problem of staggering dimensionality to a potentially tractable one and the removal of surface effects that would otherwise be troublesome for small N .

Classical statistical mechanics are performed for the periodic aggregates usually at constant temperature (T), volume (V), and N . One recent calculation on water employed the T , P , N (isothermal-isobaric) ensemble.⁷ Average values of properties, Q , for the solution at constant T , V , and N could then be calculated by determining the instantaneous value of the properties for many geometric configurations, i , of the molecules in the aggregate. These results would have to be weighted by the probability of the occurrence of each configuration as expressed by its Boltzmann factor, P_i , where E_i is the internal energy of configuration i (eq 1). In this fashion, thermodynamic functions which may be expressed as configurational averages such as the internal energy, E , or pressure can be determined.

$$\langle Q \rangle = \sum_i P_i Q_i \quad (1)$$

$$P_i = \frac{\exp(-\beta E_i)}{\sum_i \exp(-\beta E_i)}; \quad \beta = (k_B T)^{-1}$$

Characteristics of the liquid's structure may be obtained analogously. Radial distribution functions, $g(R)$, are of particular interest because they describe the variation in the distribution of solvent molecules from that which would be found in the liquid if it were uniform (structureless). For water, $g_{OO}(R)$ is related to the probability of finding an oxygen atom a distance R from another oxygen.

$$g(R) = \frac{\langle N_R(R, R + \Delta R) \rangle}{\rho 4\pi R^2 \Delta R} \quad (2)$$

It may be computed from eq 2 where the numerator is the average number of sought atoms found in the shell between R and $R + \Delta R$, ρ is the average density, N/V , and $4\pi R^2 \Delta R$ is the normalizing volume element. If the solvent distribution was uniform, then

$$\langle N_R(R, R + \Delta R) \rangle = (N/V) 4\pi R^2 \Delta R$$

and $g(R) = 1$ for all R . The distribution functions are determined experimentally by X-ray or neutron diffraction.^{3,15} The Monte Carlo results of Clementi et al. for g_{OO} of water at 25 °C are shown by the dashed line in Figure 1.⁶ The computations nearly reproduce the X-ray data of Narten et al.^{15a} Obvious features are the hydrogen bonding peak at ca. 3 Å and the existence of second and third solvation shells. Unfortunately, diffraction data are only currently available for liquid water and ammonia.¹⁵ A g_{FF} for HF(l) computed in this study is also shown in Figure 1 and will be discussed below.

Coordination numbers, C_R , are often obtained from $g(R)$ by integration to an appropriate distance, R_c ; for example, the first minimum in $g(R)$ which may be equated with the extremity of the first solvation sheath.

$$C_R = \int_0^{R_c} g(R) \rho 4\pi R^2 dR \quad (3)$$

A variety of other distribution functions may be computed. In Beveridge's study of water, distributions of coordination numbers and bonding energies are reported in terms of mole fractions of the water molecules.⁸ In the present work, the bonding energy distribution has also been determined as well as the energy pair distribution which describes the distribution of HF dimer interaction energies in the liquid. As shown here, a coordination number for HF(l) can be defined from the energy pair distribution. The result is significantly different from the value obtained from eq 3.

Other thermodynamic properties reported in this work are the heat capacity, C_v , and dielectric constant, ϵ . By differentiation of the energy equation (cf. eq 1), it is found that the heat capacity can be determined as the variance of the internal energy (eq 4). For comparisons with experiment, both the calculated energy and heat capacity must be adjusted by adding the contributions for the kinetic energy of free molecular rotations and translations. This amounts to an addition of $3RT$ to E and $3R$ to C_v for bent triatomics, and $5/2RT$ and $5/2R$ for a solution of diatomics. Corrections for quantum effects on these quantities may be estimated, and Owicki and Scheraga have done for water.⁷ Since the corrections are not great and in view of the other approximations in the MC calculations, the classical treatment is followed here.

The dielectric constant is related to the average value of the dipole moment

$$C_v = \left(\frac{\partial E}{\partial T} \right)_v = \frac{1}{k_B T^2} (\langle E^2 \rangle - \langle E \rangle^2) \quad (4)$$

squared for the entire periodic cube according to eq 5.¹⁶

$$\frac{\epsilon - 1}{\epsilon + 2} = \frac{4\pi \langle M^2 \rangle}{9V k_B T} \quad (5)$$

The statistical fluctuations in MC calculations can yield substantial error bars for the computed C_v 's. Similarly, the sensitivity of ϵ to $\langle M^2 \rangle$ for large ϵ makes reliable estimates of ϵ difficult or impossible in these cases (vide infra).

Properties such as isothermal compressibility and scattering intensities may also be computed in straightforward fashions.^{3,6} However, the free energy, A , and the entropy may not be directly evaluated by a MC calculation. Nevertheless, changes in these quantities may be obtained with some effort.^{3,17}

Selection of Configurations and Energy Evaluation. Two aspects of the evaluation of eq 1 that need further explanation are the selection of configurations and the calculation of the E_i 's. The molecules in the periodic solid are usually held fixed in their monomer geometries. The positioning, \mathbf{x}_n , of each molecule may then be specified by a six-dimensional vector composed of the location of the molecule's center of mass or another convenient point and three orientational angles (e.g., Euler angles). Naturally, spherical particles and linear mole-

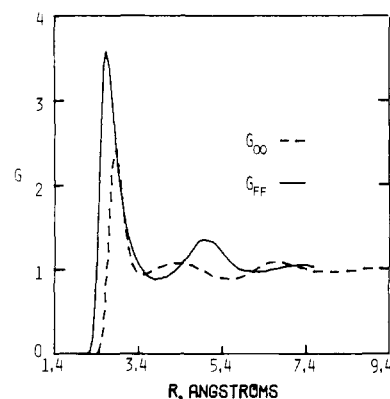


Figure 1. Comparison of the OO and FF radial distribution functions computed for water (ref 6) and liquid HF (this work).

cules require no and two angles, respectively.

$$\mathbf{x}_n = (x_n, y_n, z_n, \phi_n, \theta_n, \psi_n)$$

Thus, an entire configuration is given by

$$X_i = \mathbf{x}_1, \mathbf{x}_2, \dots, \mathbf{x}_N$$

If the configurations were chosen completely randomly (Monte Carlo), a large majority of the sampled configurations would be high in energy and cause eq 1 to be very slowly convergent. A clever elusion of this difficulty was provided by Metropolis et al.¹⁴ Simply stated, rather than sampling configurations at random and weighting the samples with their Boltzmann factors, an ordered walk may be taken in such a way that configurations occur with a probability $\exp(-\beta E_i)$. Therefore, the lower energy arrangements are sampled more heavily. The resultant configurations should then be weighted evenly which reduces eq 1 to

$$\langle Q \rangle = \frac{1}{I} \sum_{i=1}^I Q(X_i) \quad (6)$$

where I is the total number of configurations treated. For $N \leq 100$, I is usually taken to be 10^5 – 10^6 .³

A common procedure for the ordered walk is to displace a molecule from its position (x_n, y_n, z_n) in an initial configuration, X_i , to a new location $(x_n + \alpha, y_n + \beta, z_n + \gamma)$ where α , β , and γ are random numbers in an interval $(-\delta, \delta)$. For molecules, a rotation of Θ degrees about a randomly chosen axis is also performed where Θ is a random number on an interval $(-\omega, \omega)$. If the energy of the new configuration, X_{i+1} , is the same or lower than for X_i , the new configuration is accepted into the "Markov chain" and a molecule in X_{i+1} is displaced to generate X_{i+2} . If $E_{i+1} > E_i$, a random number, m , on $(0, 1)$ is picked and if $\exp[-\beta(E_{i+1} - E_i)] \geq m$, X_{i+1} is accepted. Otherwise, X_{i+1} is taken as identical to X_i and a new displacement is attempted. Metropolis et al.¹⁴ proved that this process yields the properly weighted distribution of configurations. The parameters δ and ω are selected so that a roughly 50% acceptance rate is obtained for new configurations. In general, δ is on the order of 0.2 Å and ω , 10° . The calculations are often begun with the solvent molecules arranged in a lattice reminiscent of the solid state. The first 10^5 – 10^6 configurations are then used to bring the ensemble toward equilibrium and are not counted in the averaging process.

The Monte Carlo calculations on solutions to date have predominantly employed pairwise potential functions, $E_2(\mathbf{x}_\mu, \mathbf{x}_\nu)$, to describe the configurational energy.

$$E_i \equiv E(X_i) = \sum_{\mu < \nu} E_2(\mathbf{x}_\mu, \mathbf{x}_\nu) \quad (7)$$

The energy for any configuration is then determined by the pairwise sum of the interactions between each molecule in the

Table I. Parameters in the Unscaled 12-6-3-1 Potential Function for (HF)₂ Fit to ab Initio 6-31G Energies^a

	parameter		
	FF	FH	HH
Q^2	104.025		
b	13.8785		-41.4783
c	-563.463	42.3605	59.3664
d	114169	408.745	381.556

^a Distances are in Å and energies in kcal/mol for the potential function.

image solid and surrounding molecules (eq 7). Ignoring higher order, e.g., three-body, terms appears to produce a 10–15% error (1 kcal/mol) in the computed internal energy for water, but may have little effect on the distribution functions or heat capacity.^{6,18} Computationally, determining and including higher order effects is onerous. There are two conventions for evaluating eq 7.^{13b} The most common employs a spherical cutoff (SC) such that interactions between dimers separated by more than a certain distance, usually half the cube's length, are neglected. Thus, for a given molecule only interactions with the molecules in the surrounding sphere with radius equal to half the cube's edge are evaluated. The alternative method is the minimum image (MI) procedure that is favored by Valleau.^{11a,13b} In this case, for a given molecule the interactions with the nearest images of all the other molecules in the cube are evaluated. MI calculations are slower by about a factor of 2 than SC since $N - 1$ and roughly $N/2$ interactions are considered for each molecule by the methods, respectively.¹⁹ Few comparisons have previously been made between the two procedures. Consistent with an earlier study of dipolar hard spheres,^{11a} the results presented here are found to depend noticeably on the choice of convention.

The two methods for obtaining the pair potentials may be referred to as empirical and quantum mechanical. In the empirical approach, sums of standard functions, such as Coulomb and Lennard-Jones 6:12 potentials, are parameterized to reproduce experimental properties of the monomers and dimers, e.g., dipole moment, vibrational frequencies, geometry, and hydrogen bonding energies. Many such potentials exist for the water dimer and several have been used in Monte Carlo and molecular dynamics calculations with varying success.^{3,4} The quantum mechanical approach has been pioneered by Clementi and co-workers.^{6,20} They have performed extensive ab initio molecular orbital calculations on the water dimer and water-atomic ion complexes in numerous orientations. The computed energies are then fit to an analytical expression that consists of generally recognizable terms representing Coulomb interactions and short-range repulsions for the interatomic, intermolecular interactions. The latter approach has been followed in this work using the (HF)₂ potential function obtained previously from ab initio calculations with the extended, split-valence 6-31G basis set.²

III. Computational Details

The results of three MC runs are presented in the following. For $N = 64$, both SC and MI calculations were performed in addition to an SC calculation with $N = 108$. In all cases, the computations employed a temperature of 0 °C and the experimental density (1.015 g/cm³).²¹ Therefore, the edge of the periodic cube was 12.794 Å for the 64 HF(s) and 15.232 Å for 108. The experimental value for the boiling point of liquid HF is 19.75 °C.²¹ It should be noted that HF(l) and H₂O(l) have nearly identical densities. This leads to a volume per molecule of 33 Å³ for HF(l) at 0 °C and 30 Å³ for H₂O(l) at 25 °C. Water and liquid HF also have similar, high-dielectric constants (ca. 80); however, the viscosity of HF(l) is about one-fifth that of water.²²

Each MC run was preceded by an equilibration of the system using between 300 000 and 500 000 configurations as necessary. The initial configurations were discarded and the final runs involved averaging over an additional 300 000 configurations in each case. The distance variation, δ , was in the range ± 0.17 Å and the angular variation, ω , was $\pm 10^\circ$. Random rotations were made about all three axes on each move. The limits on δ and ω provided a roughly 50% acceptance rate for new configurations.

The Potential Function. The 12-6-3-1 potential function for (HF)₂ was used throughout.² The function was obtained by fitting interaction energies calculated from ab initio 6-31G computations for 250 configurations of (HF)₂ to a simple analytic expression. The expression contains nine adjustable parameters and sixteen terms in r^{-1} , r^{-3} , r^{-6} , and r^{-12} , where r represents the four interatomic distances between atoms in the two monomers. The H-F bond lengths in the monomers have been held fixed at the experimental value (0.917 Å) in all aspects of this work. The function is given in eq 8 and the adjustable parameters are listed in Table I.

$$\begin{aligned} \Delta E(12-6-3-1) = & Q^2 \left(\frac{1}{r_{FF}} - \frac{1}{r_{FH}} - \frac{1}{r_{HF}} + \frac{1}{r_{HH}} \right) \\ & + \frac{b_{FF}}{r_{FF}^3} - \frac{1}{2} (b_{FF} + b_{HH}) \left(\frac{1}{r_{FH}^3} + \frac{1}{r_{HF}^3} \right) + \frac{b_{HH}}{r_{HH}^3} \\ & + \frac{c_{FF}}{r_{FF}^6} + c_{FH} \left(\frac{1}{r_{FH}^6} + \frac{1}{r_{HF}^6} \right) + \frac{c_{HH}}{r_{HH}^6} + \frac{d_{FF}}{r_{FF}^{12}} \\ & + d_{FH} \left(\frac{1}{r_{FH}^{12}} + \frac{1}{r_{HF}^{12}} \right) + \frac{d_{HH}}{r_{HH}^{12}} \quad (8) \end{aligned}$$

The fit of the 12-6-3-1 potential to the 6-31G energies was excellent ($\sigma = 0.38$ kcal/mol for bound dimer configurations) and the function is well-behaved, i.e., it has no extraneous minima; acyclic dimers are found to be more bound than cyclic forms, and the function has the proper long-range behavior to minimize N dependence in the MC results.²

However, a matter of concern is the predicted minimum for the dimerization energy of (HF)₂ in the gas phase. The value from the 12-6-3-1 potential is -7.57 kcal/mol which yields a dimerization enthalpy of ca. -7.2 kcal/mol.² This is in reasonable agreement with the experimental enthalpy of -6.8 ± 1 kcal/mol.²³ However, as discussed previously, there is little doubt that the experimental estimates are too low.^{2,24} The best single determinant, ab initio calculations employing large basis sets including polarization functions on fluorine and hydrogen, agree that the dimerization energy is -4.5 to -4.6 kcal/mol.²⁵ The correlation energy correction is reported to be negligible;²⁶ however, more extensive configuration interaction calculations are needed to test this point. It would seem odd if CI does not make the dimerization energy more negative as it does for (H₂O)₂ by ca. 1 kcal/mol.⁵

Another worrisome issue in simulating HF(l) is the importance of many-body effects. Specifically, Del Bene and Pople calculated that the nonadditivity of hydrogen-bond energies for head-to-tail trimers is attractive and amounts to about 1 kcal/mol per hydrogen bond.²⁷

As a consequence of these considerations, the 12-6-3-1 potential has been scaled uniformly by a factor of 0.75. This yields a predicted dimerization energy of -5.68 kcal/mol. The value embodies both a revised estimate of the true dimerization energy of (HF)₂ and some correction for three-body effects. As discussed below, the resultant energy of vaporization for HF(l) going to the ideal gas is in good agreement with experiment. Use of the unscaled 12-6-3-1 potential in a MC calculation with 64 HFs and SC imposed yields a $\Delta E^\circ_{\text{vap}}$ of 9.7 kcal/mol which is considerably larger than the experimental value, 6.7 kcal/mol.²³ Some concern must now be expressed for this experimental result since it employs the experimental dimeri-

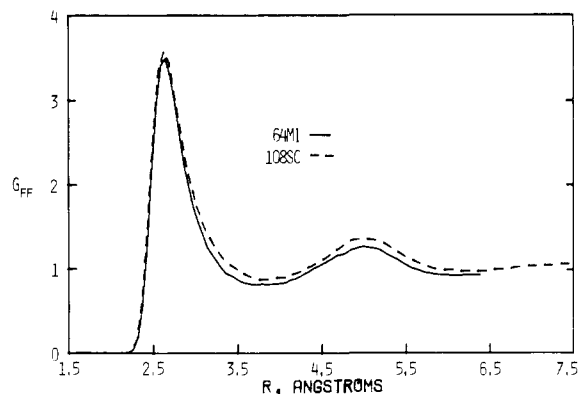
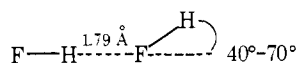


Figure 2. FF radial distribution functions computed for liquid HF.

zation enthalpy. Correction should, however, revise the number downward. It may be noted that the CI potential for $(\text{H}_2\text{O})_2$ determined by Matsuoka et al. was also adjusted post facto.^{5,6} Specifically, it was decided to neglect the intermolecular correlation energy corrections to improve the predicted hydrogen bond length and dimerization energy.^{5,6}

Another similarity between the present work and the studies of water can be found in the dipole moments for the monomers. The experimental dipole moments for HF and H_2O are 1.82 and 1.85 D, respectively.²⁸ Analysis of the Coulombic terms in the scaled 12-6-3-1 potential yields a value of 2.12 D for HF, while the CI potential for $(\text{H}_2\text{O})_2$ indicates 2.19 D for H_2O .⁶ The larger dipole moments from the potential functions are consistent with increased polarization of the monomers upon dimer formation. This effect is apparent in the 6-31G calculations for $(\text{HF})_2$. In addition, the dimerization energies from the two potential functions are close: -5.68 kcal/mol for $(\text{HF})_2$ and -5.87 for $(\text{H}_2\text{O})_2$.⁶

The geometry with lowest energy for $(\text{HF})_2$ from the 12-6-3-1 function is linear with a hydrogen bond length (1.74 Å) in fair agreement with experiment (1.79 Å).²⁹ However, ab initio calculations and experiment²⁹ predict a geometry bent by 40° – 70° .^{2,24}



The bending force constant is found to be small, so only 0.3 kcal/mol is required for the bending from linear to 40° .² Thus, this effect is not anticipated to have serious consequences on the MC calculations at 0°C . For comparison, the hydrogen bond length in the water dimer according to the CI potential is 1.91 Å.⁵ The similarities in many properties of water and hydrogen fluoride as monomers, dimers, and the pure liquids are remarkable.

IV. Results and Discussion

a. Radial Distribution Functions and the Liquid's Structure.

Results are reported for the three MC runs which are referred to as 64SC, 64MI, and 108SC. The notation indicates the number of HF molecules in the calculation and the convention used to evaluate the energy. The FF, FH, and HH radial distribution functions, $g(R)$, obtained from the scaled 12-6-3-1 potential, are shown in Figures 2–4 for the 64MI and 108SC runs. The $g(R)$ from the 64SC run are virtually identical with 64MI results except for a slightly diminished first maximum in the g_{FF} function for the 64SC computation. The locations and heights of the extrema in the radial distribution functions are compared in Table II. Estimates of the statistical errors for quantities computed in MC runs are obtained by breaking the runs into steps and observing fluctuations in the quantities between steps.^{13a} For the calculations reported here, the step size was 10 000–50 000 configurations. The resultant standard

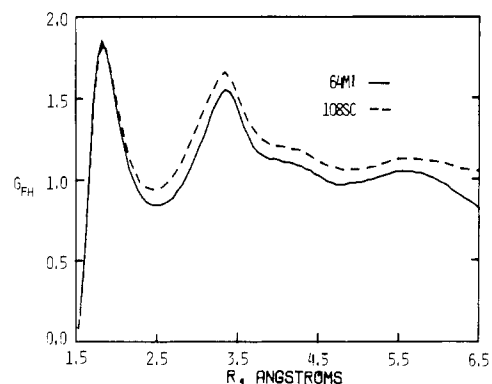


Figure 3. FH radial distribution functions computed for liquid HF.

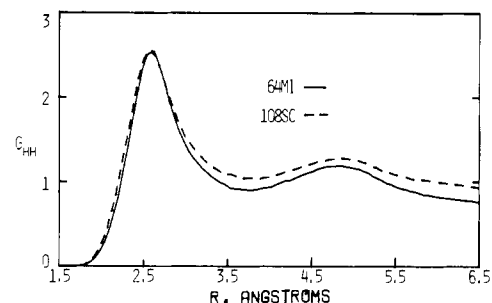


Figure 4. HH radial distribution functions computed for liquid HF.

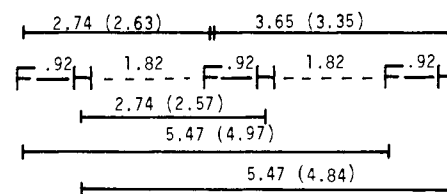


Figure 5. Analysis of peak positions in the radial distribution functions assuming linear hydrogen bonding. Setting the hydrogen bond length at 1.82 Å, the first peak in g_{FH} yields the indicated estimates for the peak positions. Values in parentheses are the actual calculated peak positions from the 108SC computation. The poor agreement argues against the appropriateness of the model.

deviations (2σ) for the $g(R)$ average 0.02–0.05 with the larger error bars for the larger values of $g(R)$. The size of the bins used to accumulate the statistics for the $g(R)$ causes the uncertainty in the R values, the locations of the extrema, to be ± 0.03 Å.

Overall, the $g(R)$ from the three runs are similar; however, slight N dependence is apparent in the SC calculations. The taller peaks in the 108SC computation than in the 64SC results indicate greater structure in the liquid as the number of molecules in the periodic cube is increased. The shift of the peak positions for g_{FF} to slightly shorter distances in the 108SC run as compared to 64SC also suggests increased bonding in the larger sample; however, the differences are not statistically significant. Nevertheless, there is a small effect on the internal energy (0.12 kcal/mol), as discussed in the next section.

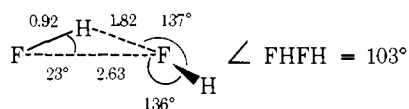
The peak positions can be analyzed to provide some idea of the structure of liquid HF. In particular, the possibility of linear hydrogen-bonded chains is considered in Figure 5. By using the HF covalent distance and assigning the hydrogen bond length as 1.82 Å (the first peak in g_{FH}), the other peak positions can readily be predicted assuming the linear model. The agreement is poor which indicates that the liquid contains dimers with significantly bent hydrogen bonds on the average. In fact, the first maxima in g_{FF} , g_{FH} , and g_{HH} , and the second

Table II. Extrema for Radial Distribution Functions at 0°C^a

function	calcn	1st max		1st min.		2nd max		2nd min.		3rd max	
		r	g	r	g	r	g	r	g	r	g
g _{FF}	64SC	2.65	3.20	3.86	0.81	5.01	1.24	6.11	0.90		
	64MI	2.65	3.49	3.86	0.81	5.01	1.26	6.11	0.92		
	108SC	2.63	3.58	3.80	0.87	4.97	1.35	6.27	0.97	7.38	1.06
g _{FH}	64SC	1.82	1.80	2.48	0.78	3.42	1.49	4.96	0.99	5.62	1.05
	64MI	1.82	1.86	2.48	0.84	3.36	1.56	4.79	0.97	5.56	1.06
	108SC	1.82	1.84	2.44	0.95	3.35	1.66	4.91	1.06	5.56	1.13
g _{HH}	64SC	2.54	2.34	3.75	0.95	4.68	1.14				
	64MI	2.59	2.53	3.80	0.90	4.85	1.20				
	108SC	2.57	2.56	3.74	1.04	4.84	1.28				

^a r in Å and g are the location and height of the maxima and minima. The error limits on r are ±0.03 Å and on g ±0.02 to ±0.05.

maximum in g_{FH}, can be used to construct an *average* structure for the dimers in the liquid:



This picture is consistent with displays of numerous configurations of the periodic cubes that have been made on a Texas Instruments 990/10-Tektronix computer system. The liquid consists of long, twisting chains of hydrogen-bonded monomers. Adjacent chains tend to run in opposite directions which keeps the dipole moment of the cube low. The occurrence of cyclic polymers is not pronounced. It is difficult to present lucid drawings of the periodic cubes here, since the ability of the computer graphics terminal to rotate the display is not available. However, some of the hydrogen-bonded chains can be extracted from the cube and displayed in two dimensions. Figure 6 has been prepared in this fashion using a low-energy configuration from the 64MI calculation. Clearly, the 12-6-3-1 potential's preference for linear hydrogen bonds does not have dramatic influence on the structural results.

A consistent difference in Figures 2-4 is that the $g(R)$ from the 108SC run are uniformly above the 64MI results beyond the first maxima. This implies a higher local density in the larger sample. Thus, the number of HF(s) under the g_{FF} out to 6 Å are 32.4 and 30.1 for the 108SC and 64MI calculations. Similar results were obtained in simulations of HF(l) with an earlier 12-3-1 potential in 64SC and 108SC runs; however, the $g(R)$ were essentially constant in 108SC and 216SC calculations. In any event, the local density in the calculations seems too high because 27 molecules would be expected out to 6 Å assuming uniform density. The problem also appears to be reflected in the recurrence of sparsely populated regions in the displays of the periodic cubes. Thus, the results presented here must be tempered with this concern. If the problem is real, improvements in the potential function could hopefully eradicate it. However, there is always the nagging question of the ultimate importance of three-body and higher order effects.³⁴

It should be noted that the structure of the liquid is reminiscent of the X-ray results for solid HF determined by Atoji and Lipscomb.³⁰ They found that the crystals consist of parallel "infinite zigzag chains of hydrogen bonds" with a hydrogen bond angle about fluorine of 120°. The FF separation of 2.49 ± 0.01 Å in the solid can be compared with the location of the first peak in g_{FF} for the liquid (2.63 Å). The discrepancy is in accordance with the much higher density of the solid (1.663 g/cm³) at the experimental temperature (-125 °C)³⁰ than the density of the liquid at 0 °C (1.015 g/cm³).

The g_{FF} for the 108SC calculation is shown in Figure 1 with the g_{OO} for water from Clementi's SC calculation using the CI potential.⁶ The simulations reveal several well-defined peaks

which are generally associated with solvation shells. Interestingly, the height and breadth of the first two peaks for HF(l) are much greater than for water, although the hydrogen bond energies and densities are similar. Consequently, the coordination number for HF in the liquid is between 8 and 9 from all three MC calculations when g_{FF} is integrated up to its first minimum (ca. 3.9 Å). The coordination number for water is 4-5, as expected.^{6,8} Further analysis of the MC results shows that the high coordination number for HF results largely from contributions of HF(s) in adjacent chains. As discussed below, the energy pair distribution reveals that each HF is only strongly hydrogen bonded to an average of two neighboring molecules in agreement with chemical intuition. The discrepancy is related to the fact that the concept of a solvation shell for a "linear" liquid like HF consisting of hydrogen-bonded chains is not as clearly defined as for spherical liquids (e.g., noble gas liquids) or for liquids whose three-dimensional structure renders them pseudospherical (e.g., water).

To complete this discussion of coordination numbers, it is noted that all three MC runs find ca. 1.75 hydrogens under the first peak of g_{FH} . One may clearly be assigned to a strongly hydrogen-bonding neighbor, while the remainder involves contact from other chains within 2.5 Å. If liquid HF consisted of perfectly linear, parallel chains, a simple calculation shows that the distance between chains would be 3 Å. Obviously, it would be most desirable to compare the MC results presented here with diffraction data. Without this information, it is difficult to assess the utility of the 12-6-3-1 function or any other potential for simulating liquid HF. Hopefully, this study will expedite the experimental work.

The results presented here can be compared to the recent molecular dynamics work of Klein et al.^{9b} Fortunately, all simulations have been performed at about 0 °C and with the same density (1 g/cm³). These authors have used both a central force potential derived from experimental data on the HF monomer and dimer and a potential derived from the ab initio calculations of Schaefer et al.^{25a} The structural results from the MC calculations and the molecular dynamics (MD) run with the central force potential are similar except the first peak in g_{FF} is slightly split in the MD study. Thus, the MD results appear to distinguish the two strongly hydrogen bonded neighbors from the peripheral contacts more than the MC description. The MD run with the ab initio potential yields much less structure than the other studies. The only thermodynamic datum that can be compared is the internal energy. The results are consistent with the well depths for the different dimer potentials; the MC prediction (-6.9 kcal/mol, vide infra) is lower than the MD results (-5.6 and -6.2 kcal/mol). It would be interesting to study in detail the effect of the well depth on the shape of the first peak in g_{FF} .

b. Thermodynamic Properties. Energetics. The results of the calculations for the energy, heat capacity, energy of vaporization, and $\langle M^2 \rangle$ are assembled in Table III. The energy, E ,

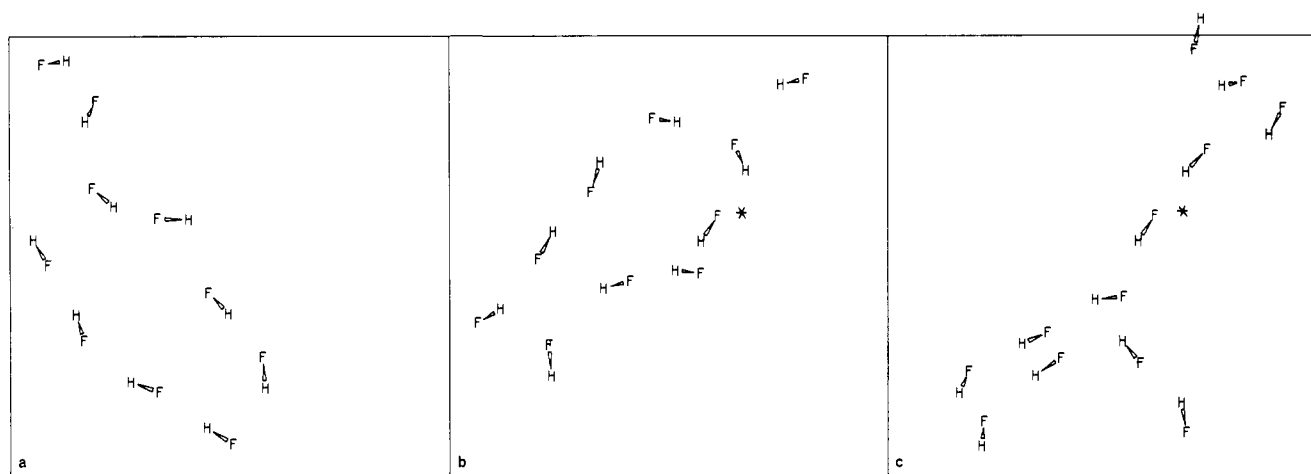


Figure 6. Examples of hydrogen-bonded chains extracted from a low-energy configuration in the 64 MI calculation. The border in the three drawings represents the edges of the periodic cube. The illustrated molecules are all unique except the starred molecule in Figures 6b and 6c is the same. Thus, 31 of the 64 molecules are shown. Figures 6a and 6b reveal the general trend for adjacent chains to run in opposite directions.

Table III. Calculated Thermodynamic Properties for Liquid HF.^a

calcn	$-E_i$	$-E$	C_v	$\Delta E^\circ_{\text{vap}}$	$\langle M^2 \rangle$
64SC	6.86	5.50	12.5	6.73	87.5
64MI	7.41	6.05	12.7	7.26	57.3
108SC	6.98	5.62	11.8	6.85	91.8

^a Energies in kcal/mol; C_v in cal/mol K; $\langle M^2 \rangle$ in D². All measurements refer to 0 °C except $\Delta E^\circ_{\text{vap}}$ which is at the boiling point, 19.75 °C. E_i is the internal potential energy. E and C_v include the classical kinetic energy contributions. $\Delta E^\circ_{\text{vap}}$ is the energy of vaporization for the liquid going to the ideal gas. Standard deviations for the energies, C_v and $\langle M^2 \rangle$, are ca. 0.05 kcal/mol, 1.8 cal/mol K, and 24 D².

and C_v have been corrected for the classical kinetic energy contributions, as discussed above. The energy of vaporization, $\Delta E^\circ_{\text{vap}}$, refers to converting the liquid to the ideal gas at the boiling point, 19.75 °C. It has been calculated according to eq 9. The net result of the computation is that $\Delta E^\circ_{\text{vap}}$ is essentially the negative of the internal energy of the liquid.

$$\Delta E^\circ_{\text{vap}} = E^{19.75^\circ}(\text{ideal gas}) - E^{19.75^\circ}(\text{l}) \quad (9)$$

$$E^{19.75^\circ}(\text{l}) = E^{0^\circ}(\text{l}) + \int_0^{19.75^\circ} C_v dT \approx E^{0^\circ}(\text{l}) + 19.75 C_v$$

$$E^T(\text{ideal gas}) = \frac{5}{2} RT$$

The standard deviations (2σ) for the thermodynamic properties are roughly 0.05 kcal/mol for the energies, 1.8 cal/mol K for C_v and 24 D² for the mean-squared polarization of the periodic cube.

A slight N dependence is apparent in the SC results; the energy decreases by 0.12 kcal/mol upon increasing the sample size from 64 to 108. Part of the difference is attributable to the imbalance in the r^{-6} terms in the 12-6-3-1 potential, i.e., $c_{FF} + 2c_{FH} + c_{HH} \neq 0$.² The effect can be estimated from eq 10 where r_1 and r_2 are the cutoff radii for the 64SC and 108SC computations and Δc is the imbalance in the coefficients.

$$\Delta E = \int_{r_1}^{r_2} 4\pi r^2 \rho \Delta c r^{-6} dr \quad (10)$$

The result is that 0.06 of the 0.12 kcal/mol can be accounted for in this manner. Although the remainder is within the statistical error limits for the calculations, the differences in the radial distribution functions for the 64SC and 108SC runs also indicate that there is probably some increase in order apparent in the larger sample. This conclusion is consistent with the results of Levesque et al. for dipolar hard spheres.^{11b} Slight N dependence is apparent in their data at the largest dipole moment that was employed. It should be noted that the largest dipole moment in the studies by Levesque and Valteau corresponds to only 1.0–1.5 D.¹¹ Remarkably, a complete lack of

N dependence has been reported in the MC simulations of water for $N = 27$ –343 in spite of the monomer's dipole moment.^{6,8,20} Further study of this issue is in progress.

A correction to the energy of the 108SC calculation due to distant molecules can be made from eq 10 by integrating from the cutoff to infinity. This amounts to only -0.09 kcal/mol. Additional corrections for dispersion and dipole-dipole interactions with molecules beyond the cutoff can also be made.^{3b,7,11b} For water these effects have been estimated to total ca. -0.15 kcal/mol when $N = 64$.⁷ Considering the nature of the potential functions, the treatment of many-body effects, and the statistical fluctuations in MC calculations, the corrections do not have great importance.

The most intriguing result in Table III is the low potential energy found in the 64MI calculation (-7.41 kcal/mol). The effect is again consistent with the observations of Levesque et al.^{11b} The result is not entirely due to increasing the number of interactions that are evaluated. Thus, in going from the 64SC to 108SC calculation the average number of dimer interactions considered increases from about 37 to 60 and the energy drops 0.12 kcal/mol. However, in going from 108SC to 64MI the number of interactions only differs by roughly 3 (60 vs. 63), but the energy decreases an additional 0.4 kcal/mol. There is unquestionably a fundamental difference between the MI and SC results. The first notion was that ergodic difficulties may have been encountered in the SC calculations, i.e., they were stuck in local minima in configuration space. This possibility was examined by beginning a 64SC run from a low-energy 64MI configuration. The configuration had a potential energy of -6.67 kcal/mol when evaluated by the MI convention and -7.28 kcal/mol using SC. The energy rose to -6.9 kcal/mol within 15 000 configurations of the 64SC run.³¹ As stated by Valteau,^{13b} comparisons of MI and SC results certainly warrant further attention. No MI calculations for water have been reported so far. This problem is also under investigation.

As stated previously, the computed $\Delta E^\circ_{\text{vap}}$ from the SC

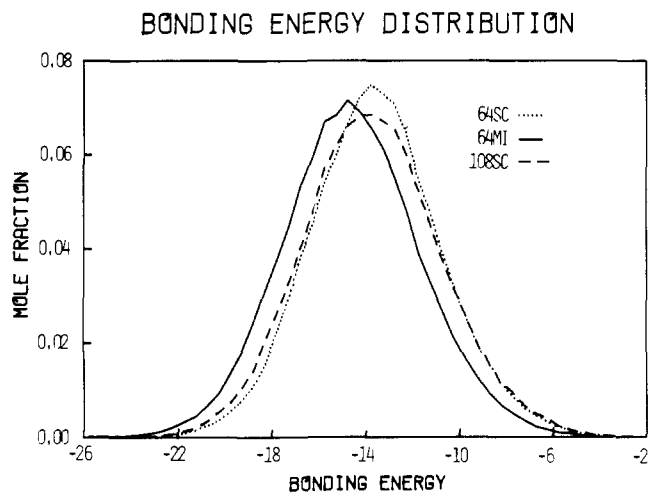


Figure 7. Calculated bonding energy distribution for the monomers in liquid HF. The data were collected in bins 0.5 kcal/mol wide. The mole fraction of the molecules in each bin is shown on the y axis.

runs, 6.73 and 6.85 kcal/mol, are in good agreement with the available experimental value, 6.7 kcal/mol.²³ The energy of vaporization for the liquid going to the real gas, ΔE_{vap} , is much smaller (1.7 kcal/mol) due to the substantial association of the gas into dimers and higher polymers.²³

Heat Capacity and Dielectric Constant. The calculated heat capacities for the three MC runs are similar (ca. 12 cal/mol K, Table III). Unfortunately, no experimental value for C_v is available. However, several reports have been made for C_p , though the correct value is a matter of debate.³² It appears that $11 < C_p < 17$ at 0 °C.³² Since C_v is anticipated to be somewhat lower than C_p , the upper end of the range for C_p is consistent with the computed C_v . The C_v of 12 for HF(l) at 0 °C is also reasonable in view of the C_v of 18 for water at 25 °C.³³ The order agrees with the lower energy for water (-8.1 kcal/mol³³) than HF (ca. -6 kcal/mol, Table III). The high C_v for water is generally attributed to its three-dimensional structure, while the lower C_v for HF(l) is in accord with its chain-like, less-branched character. The lower viscosity for HF(l) than water presumably has the same origins.

Estimates of $\langle M^2 \rangle$ can be obtained from eq 5 and the experimental dielectric constant for HF(l) at 0 °C (80²²). The predicted values for $N = 64$ and 108 are 54.5 and 92.0 D² which agree with the 64MI and 108SC values in Table III. However, the calculated $\langle M^2 \rangle$ cannot be used to estimate ϵ due to the uncertainties (± 24 D²) in the calculated $\langle M^2 \rangle$ and the sensitivity of ϵ to $\langle M^2 \rangle$ in eq 5. For example, although the difference in $\langle M^2 \rangle$ for the 64MI run and experiment is only 2.5 D², the calculated $\langle M^2 \rangle$ leads to a negative estimate for ϵ . The use of eq 5 in MC calculations to estimate large dielectric constants is clearly hopeless. Amusingly, the $\langle M^2 \rangle$ from the 108SC calculation yields an ϵ of 79.7.

c. Energy Distribution Functions. The distribution of binding energies for HF(l) is shown in Figure 7. The ordinate indicates the mole fraction of HF monomers that have the binding energy indicated on the abscissa. The distributions are centered at about -14 kcal/mol for the SC calculations and at -15 kcal/mol for the 64MI run. These values are in accord with twice the corresponding potential energies since two molecules are involved in each interaction. Furthermore, since the hydrogen bond energy from the 12-6-3-1 potential is -5.7 kcal/mol, the distributions suggest a net of 2–3 hydrogen bonds per molecule. The energy pair distribution provides additional insights, as discussed below.

The shapes of the distributions for all three MC calculations are similar. There is a smooth distribution of energies over an ca. 20 kcal/mol range. Thus, *the monomers in liquid HF ex-*

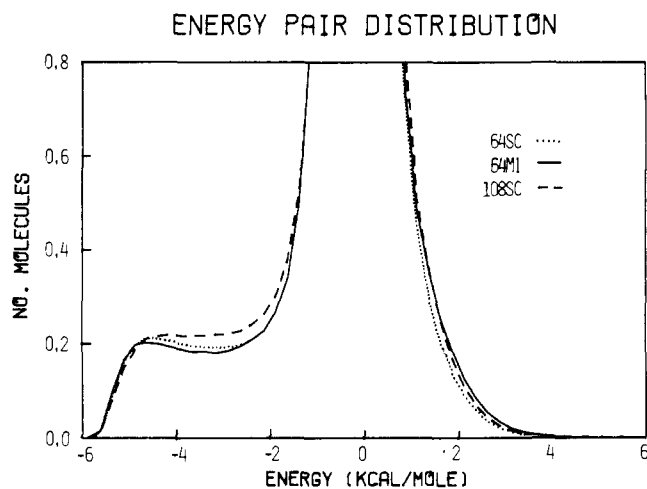


Figure 8. Calculated distributions of dimerization energies in liquid HF. The data were collected in bins 0.25 kcal/mol wide. The average number of molecules found in each bin is shown on the y axis.

perience a smoothly varying spectrum of energetic environments. This result is consistent with a "continuum" model for liquid HF. Analogous results have been obtained by Swaminathan and Beveridge for liquid water.⁸ The energy distribution for the CI potential was found to be centered at -17.7 kcal/mol.⁸

The energy pair distributions for the calculations are shown in Figure 8. In this case, the ordinate shows the average number of molecules that are bound to an HF monomer in the liquid with the energy given on the abscissa. Clearly, there may be no interaction energies below -5.7 kcal/mol. The results are again very similar. Some important observations can be made from the figure.

(1) The smaller number of highly bonding interactions for the 64MI calculation shows that this is not the region responsible for the lower potential energy of this run. Further analysis of the distribution indicates the energetic gain in the 64MI run occurs in the ± 1 kcal/mol range for interaction energies which is off-scale in the figure. For example, the number of interactions that have $-1 < \Delta E < 0$ for the 64MI and 64SC runs are 36.4 and 20.9. Thus, the evidence indicates more long-range order in the MI calculation.

(2) The distributions in Figure 8 show shallow minima at -2.89 and -3.13 kcal/mol for the 64SC and 64MI runs. Although there is no minimum for the 108SC calculations, all three distributions are fairly flat from ca. -4.9 to -2.4 kcal/mol. Integrating the distribution from -6.0 to -3.0 and to -2.5 kcal/mol reveals that there are 1.8 and 2.2 molecules in these ranges. Therefore, *the number of molecules that are strongly hydrogen bonded to an HF in the liquid is ca. 2.* This provides an alternative estimate for the coordination number. The value of 8–9 obtained from g_{FF} clearly includes many peripheral interactions. Overall, the energy pair distribution is highly informative and should be reported in more molecular dynamics and MC studies.

Conclusion. The results of Monte Carlo simulations of liquid hydrogen fluoride at 0 °C have been analyzed here to gain insights into the fluid's structure. The liquid consists of winding, hydrogen-bonded chains. The interactions between chains contribute constructively to the energy and a continuum of energetic environments are experienced by the HF monomers in the liquid. The coordination number was studied in two ways. The traditional method for its evaluation from the FF radial distribution function leads to a value of 8–9, while a new definition based on the energy pair distribution yields a coordination number of 2. The computed thermodynamic properties are in reasonable agreement with the available experi-

mental data. It is hoped that this study will stimulate further experimental examination of liquid HF and (HF)₂ in the gas phase in order to provide more reliable bases for comparisons with theory. Diffraction data on HF(l) and reexamination of the dimerization energy for HF are particularly desirable.

Several computational issues have been addressed. The small *N* dependence in the SC results for samples of 64 and 108 HF(s) finds precedent in the simulations of water. This provides further assurance that MC calculations are indeed capable of treating systems involving intermolecular interactions as strong as hydrogen bonding. Nevertheless, extension to aggregates with even stronger attractive forces, e.g., ionic solutions, must be approached with caution in view of the potential importance of many-body effects.

An intriguing observation is the significant dependence of the energy for the calculations with 64 HF(s) on the convention used to evaluate the intermolecular interactions, spherical cutoff, or minimum image. Although these results are consistent with earlier work on dipolar hard spheres, additional comparisons with larger sample sizes are warranted. The source of the difference was attributed to greater long-range order in the MI calculations. The question of which method, SC or MI, is the more proper (or less improper) also deserves further consideration.

Acknowledgments. The author is grateful to the following scientists for many helpful discussions and insights into the execution of the calculations reported here: Drs. D. L. Beveridge, A. Rahman, F. H. Stillinger, and J. P. Valleau. Receipt of preprints^{9b} from Dr. McDonald is appreciated. Computational assistance in generating the figures was kindly provided by Mr. Dean Jagels. Acknowledgment is made to the donors of the Petroleum Research Fund, administered by the American Chemical Society, for support of this work. Additional aid was provided by the Purdue Research Foundation and the Purdue University Computing Center. Gratitude is also expressed to Research Corporation for partial support of the TI990/10 computing system and graphics facility.

References and Notes

- (1) Quantum and Statistical Mechanical Studies of Liquids. 2. Part 1: ref 2.
- (2) W. L. Jorgensen and M. E. Cournoyer, *J. Am. Chem. Soc.*, **100**, 4942 (1978).
- (3) For reviews, see: (a) J. A. Barker and D. Henderson, *Rev. Mod. Phys.*, **48**, 587 (1976); (b) R. O. Watts and I. J. McGee, "Liquid State Chemical Physics", Wiley, New York, N.Y., 1976.
- (4) (a) A. Rahman and F. H. Stillinger, *J. Chem. Phys.*, **55**, 3336 (1971); (b) A. Rahman, F. H. Stillinger, and H. L. Lemberg, *ibid.*, **63**, 5223 (1975); (c) F. H. Stillinger and A. Rahman, *ibid.*, **68**, 666 (1978).
- (5) O. Matsuoka, E. Clementi, and M. Yoshimine, *J. Chem. Phys.*, **64**, 1351 (1976).
- (6) G. C. Lie, E. Clementi, and M. Yoshimine, *J. Chem. Phys.*, **64**, 2314 (1976).
- (7) J. C. Owicki and H. A. Scheraga, *J. Am. Chem. Soc.*, **99**, 7403 (1977).
- (8) S. Swaminathan and D. L. Beveridge, *J. Am. Chem. Soc.*, **99**, 8392 (1977).
- (9) (a) I. R. McDonald and M. L. Klein, *J. Chem. Phys.*, **64**, 4790 (1976); (b) M. L. Klein, I. R. McDonald, and S. F. O'Shea, *ibid.*, in press; I. R. McDonald and M. L. Klein, in press; (c) G. D. Harp and B. J. Berne, *Phys. Rev. A*, **2**, 975 (1970); J. Barojas, D. Levesque, and B. Quentrec, *ibid.*, **7**, 1092 (1973).
- (10) D. J. Evans and R. O. Watts, *Mol. Phys.*, **32**, 93 (1976).
- (11) (a) G. N. Patey and J. P. Valleau, *J. Chem. Phys.*, **61**, 534 (1974); (b) D. Levesque, G. N. Patey, and J. J. Weis, *Mol. Phys.*, **34**, 1077 (1977).
- (12) For a review, see: D. M. Brouwer and H. Hogeveen, *Prog. Phys. Org. Chem.*, **9**, 179 (1972).
- (13) (a) W. W. Wood in "Physics of Simple Liquids", H. N. V. Temperley, J. S. Rowlinson, and G. S. Rushbrooke, Eds., Wiley-Interscience, New York, N.Y., 1968; (b) J. P. Valleau, S. G. Whittington, and G. M. Torrie in "Statistical Mechanics", Part A, B. J. Berne, Ed., Plenum Publishing Co., New York, N.Y., 1977.
- (14) N. Metropolis, A. W. Rosenbluth, M. N. Rosenbluth, A. H. Teller, and E. Teller, *J. Chem. Phys.*, **21**, 1087 (1953).
- (15) (a) A. H. Narten, M. D. Danford, and H. A. Levy, *Discuss. Faraday Soc.*, **43**, 97 (1967); (b) A. H. Narten, *J. Chem. Phys.*, **66**, 3117 (1977).
- (16) This is a somewhat controversial relation. See ref 11 for details.
- (17) The free energy of water has recently been calculated by MC methods: M. Mezei, S. Swaminathan, and D. L. Beveridge, *J. Am. Chem. Soc.*, **100**, 3255 (1978).
- (18) (a) B. R. Lentz and H. A. Scheraga, *J. Chem. Phys.*, **58**, 5296 (1973); (b) S. R. Ungemach and H. F. Schaefer III, *J. Am. Chem. Soc.*, **96**, 7898 (1974).
- (19) For an MI calculation with *N* = 100 and a total of 10⁶ configurations, the number of dimer interactions that would be evaluated is 10⁶ × 99 ≈ 10⁸ since only one molecule is moved per configuration. Nevertheless, this is what makes MC calculations costly. It also necessitates great care in the selection and programming of the potential functions.
- (20) H. Popkie, H. Kistenmacher, and E. Clementi, *J. Chem. Phys.*, **59**, 1325 (1973).
- (21) I. Sheft, A. J. Perkins, and H. H. Hyman, *J. Inorg. Nucl. Chem.*, **35**, 3677 (1973).
- (22) M. Kilpatrick and J. G. Jones in "The Chemistry of Non-aqueous Solvents", Vol. 2, J. J. Lagowski, Ed., Academic Press, New York, N.Y., 1967, p 43.
- (23) C. E. Vanderzee and W. W. Rodenburg, *J. Chem. Thermodyn.*, **2**, 461 (1970).
- (24) P. A. Kollman in "Applications of Electronic Structure Theory", H. F. Schaefer III, Ed., Plenum Press, New York, N.Y., 1977, p 109.
- (25) (a) D. R. Yarkony, S. V. O'Neil, H. F. Schaefer III, C. P. Baskin, and C. F. Bender, *J. Chem. Phys.*, **60**, 855 (1974); (b) G. H. F. Diercksen and W. P. Kraemer, *Chem. Phys. Lett.*, **6**, 419 (1970).
- (26) H. Lischka, *J. Am. Chem. Soc.*, **96**, 4761 (1974).
- (27) J. E. Del Bene and J. A. Pople, *J. Chem. Phys.*, **55**, 2296 (1971).
- (28) R. D. Nelson, D. R. Lide, and A. A. Maryott, *Natl. Stand. Ref. Data Ser., Natl. Bur. Stand., No. 10* (1967).
- (29) T. R. Dyke, B. J. Howard, and W. Klemperer, *J. Chem. Phys.*, **56**, 2442 (1972).
- (30) M. Atoji and W. N. Lipscomb, *Acta Crystallogr.*, **7**, 173 (1954).
- (31) The 64SC run did show some oscillation between configurations with total energies of roughly -440 and -425 kcal/mol.
- (32) A. L. Horvath, *Z. Phys. Chem. (Frankfurt am Main)*, **78**, S209 (1972), and references therein.
- (33) N. E. Dorsey, "Properties of Ordinary Water-Substance", Reinhold, New York, N.Y., 1940.
- (34) The simulations of water have also been plagued with difficulties in reproducing the experimental pressure and density.^{4,6-8}